

Supporting Information for:

“Sources and mixing state of size-resolved elemental carbon particles in a European megacity: Paris”

Robert M. Healy¹, Jean Sciare², Laurent Poulain³, Katharina Kamili³, Maik Merkel³, Thomas Müller³, Alfred Wiedensohler³, Sabine Eckhardt⁴, Andreas Stohl⁴, Roland Sarda-Estève², Eoin McGillicuddy¹, Ian P. O’Connor¹, John R. Sodeau¹, John C. Wenger¹

¹Department of Chemistry and Environmental Research Institute, University College Cork, Ireland

²LSCE, Laboratoire des Sciences du Climat et de l’Environnement, CEA-CNRS-UVSQ, Gif-sur-Yvette, France

³Leibniz Institute for Tropospheric Research, Leipzig, Germany

⁴Norsk Institutt for Luftforskning, Kjeller, Norway

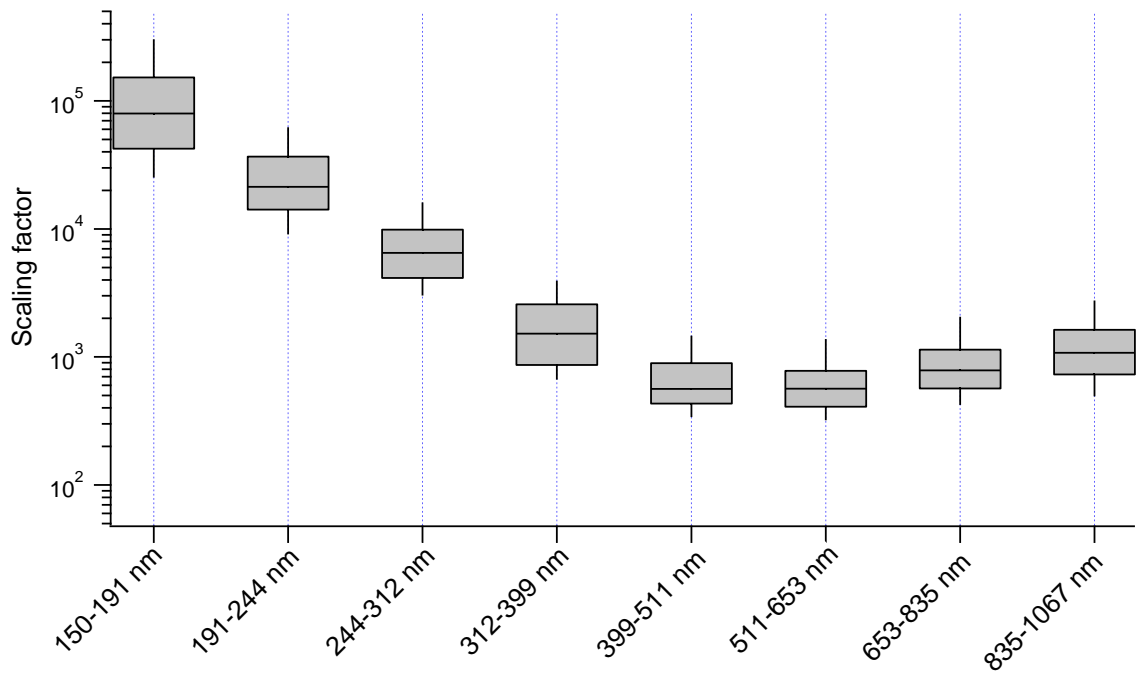


Fig. S1: Box-plot of hourly size-dependent scaling factors for the entire measurement period ($n = 624$). Median, 75th percentile and 90th percentile are denoted by the solid line, box and whisker respectively.

Scaling Procedure:

The scaling factors employed here were observed to be strongly dependent upon particle size, but the magnitude of the factors is similar to that observed in previous studies involving the use of laser particle counters, aerodynamic particle sizers and scanning mobility particle sizers to scale ATOFMS particle number concentrations (Wenzel et al., 2003; Qin et al., 2006; Pratt et al., 2009). The size bin width was generated by merging adjacent pairs of TDMPS size bins because the original size bins were found to be too narrow, resulting in low ATOFMS hourly counts in some bins during certain periods of the measurement campaign. The uncertainty associated with the TDMPS particle number concentrations in the size range used here (100-712 nm, mobility diameter) is estimated to be < 2% (Birmili et al., 1999). The bins used are wider than those used previously by Pratt et al (2009) but narrower than those used by Wenzel et al (2003) and Qin et al (2006). The bin width was not increased any further because, although this would reduce the magnitude of the scaling factors required, information on the size-dependence of the elemental carbon particle mass associated with different sources would be lost.

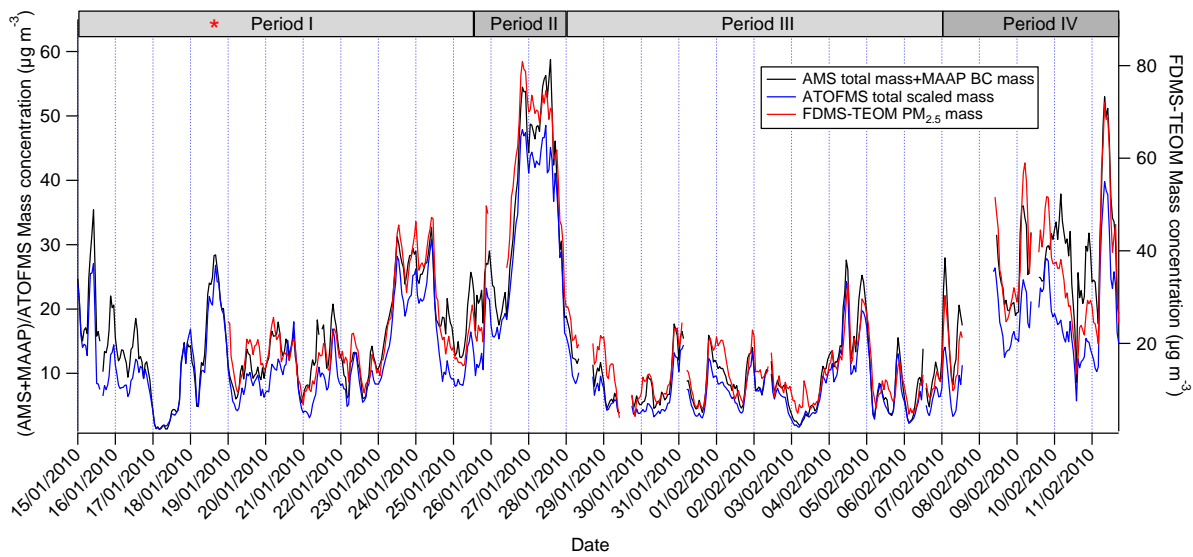


Fig. S2: ATOFMS total scaled particle mass concentration (150-1067 nm, d_{va} , left axis), sum of AMS total mass (ammonium + chloride + nitrate + sulfate + organics) + MAAP BC mass concentration (left axis), and FDMS-TEOM PM_{2.5} mass concentration (right axis).

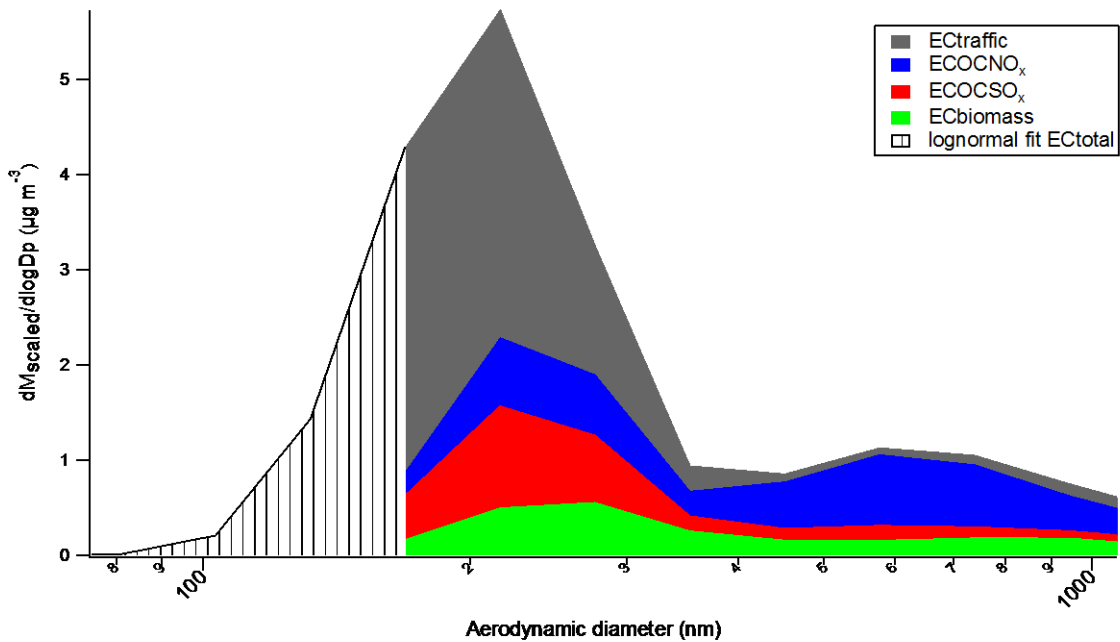


Fig. S3: Lognormal fit of the average scaled ATOFMS mass size distribution for EC particles extrapolated below 150 nm. Only the the size bins covering the size range of the smaller mode (150-400 nm) were used to generate the lognormal curve. The mass contribution below 150 nm is ~9% of the total.

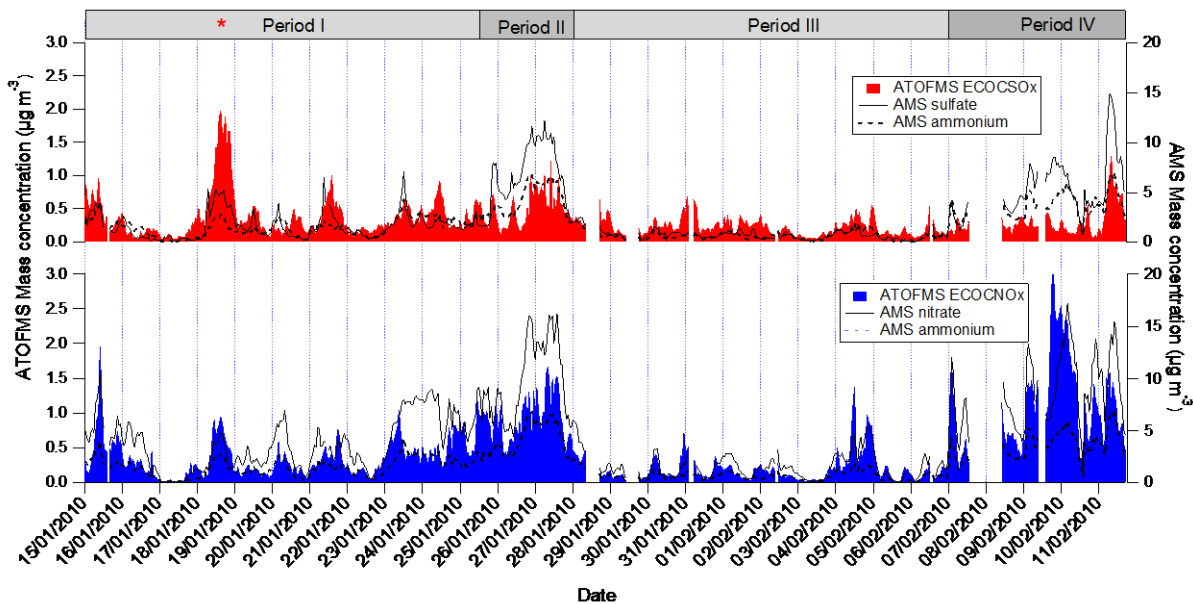


Fig. S4: ATOFMS scaled mass concentration for ECOCSO_x and ECOCNO_x particles (left axis) compared with mass concentrations of ammonium, nitrate and sulfate from the AMS (right axis).

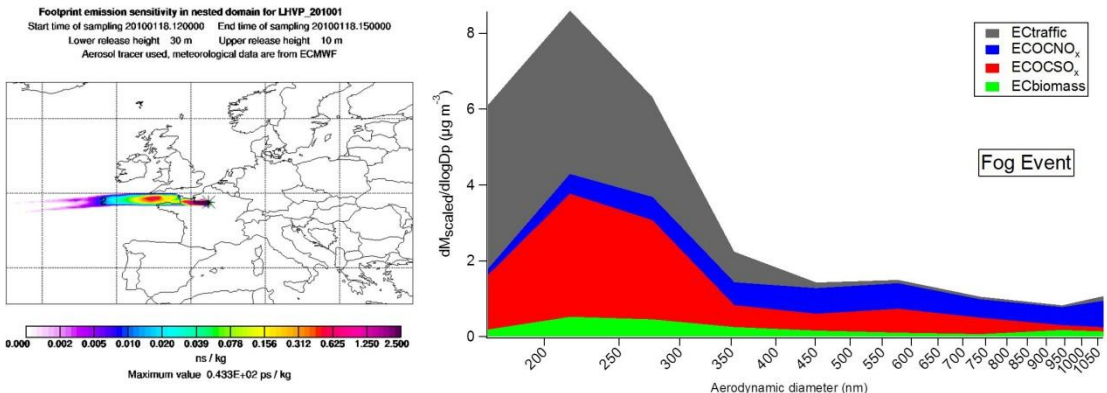


Fig. S5: Potential emission sensitivity (left) and average mass size distribution for the 4 ATOFMS EC classes (right) on 18/01/2010. The numbers in the potential emission sensitivity plot corresponds to the air mass age in days, and are positioned on the centroid of the retroplume position at that time.

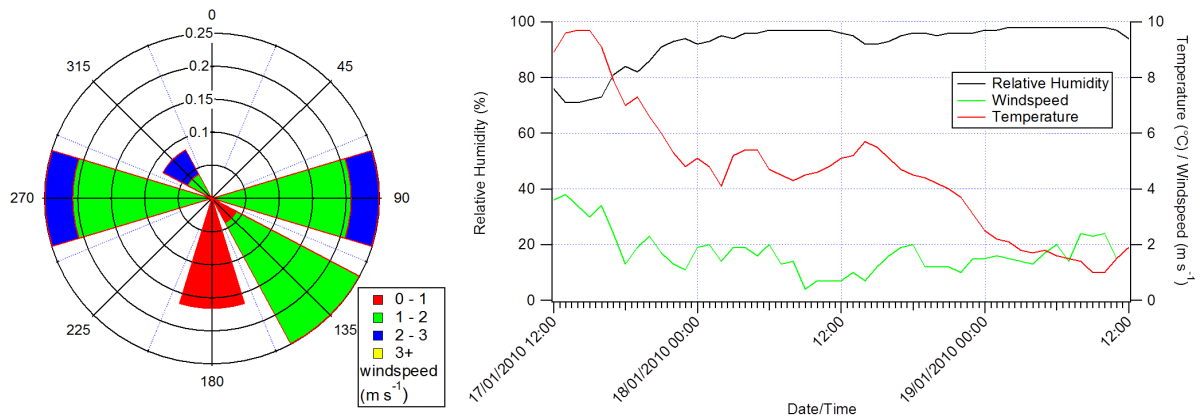


Fig. S6: Windrose for 18/01/2010 (left) and meteorological data for the period of interest (right). Meteorological data provided by Meteo France, Parc Montsouris, ($48^{\circ}49'18\text{N}$, $2^{\circ}20'12\text{E}$, 75m a.s.l.), approximately 1.5 km from LHVP.



Fig. S7: Photograph taken at LHVP at 11:30 on 18/01/2010

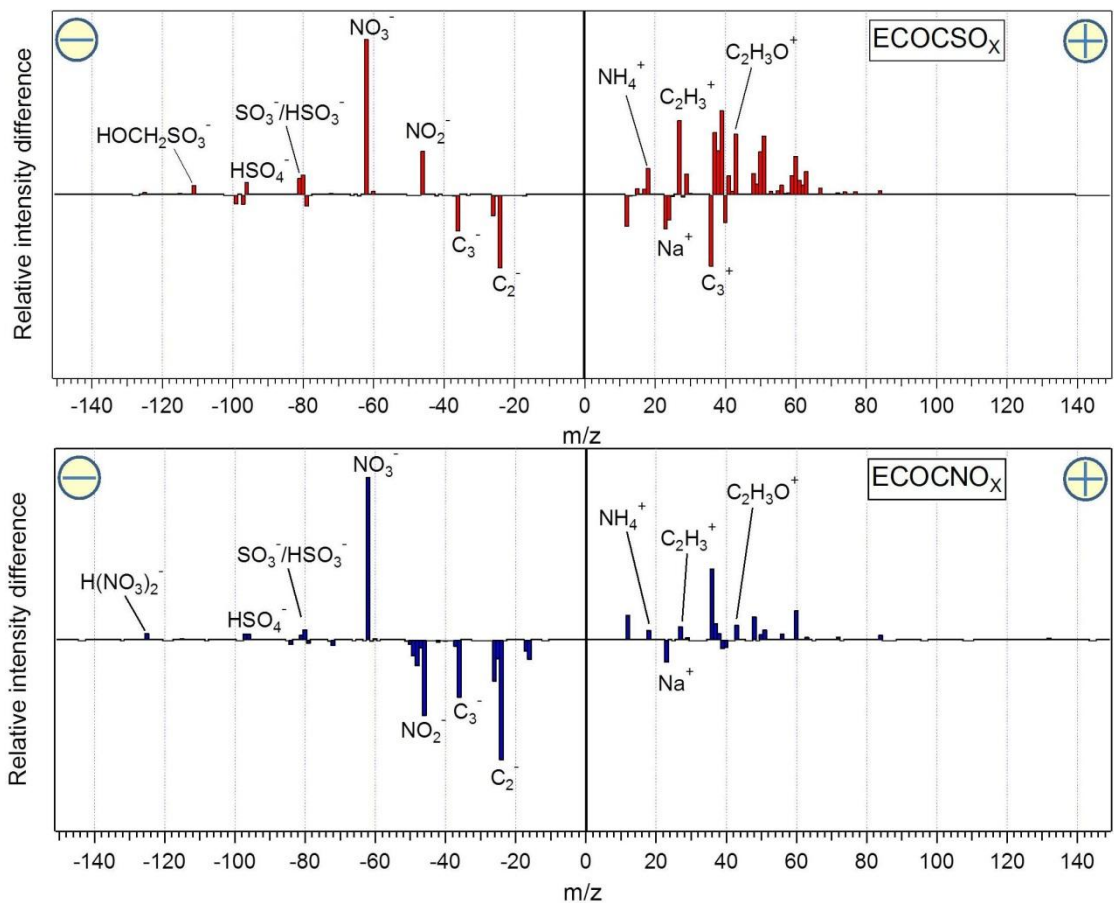


Fig. S8: Difference mass spectra for ECOC SO_x (top) and ECOC NO_x (bottom) particles below and above 400 nm (d_{va}) on 18/01/2010. Relative intensity difference above the line indicates enhancement of these species in the larger particles.

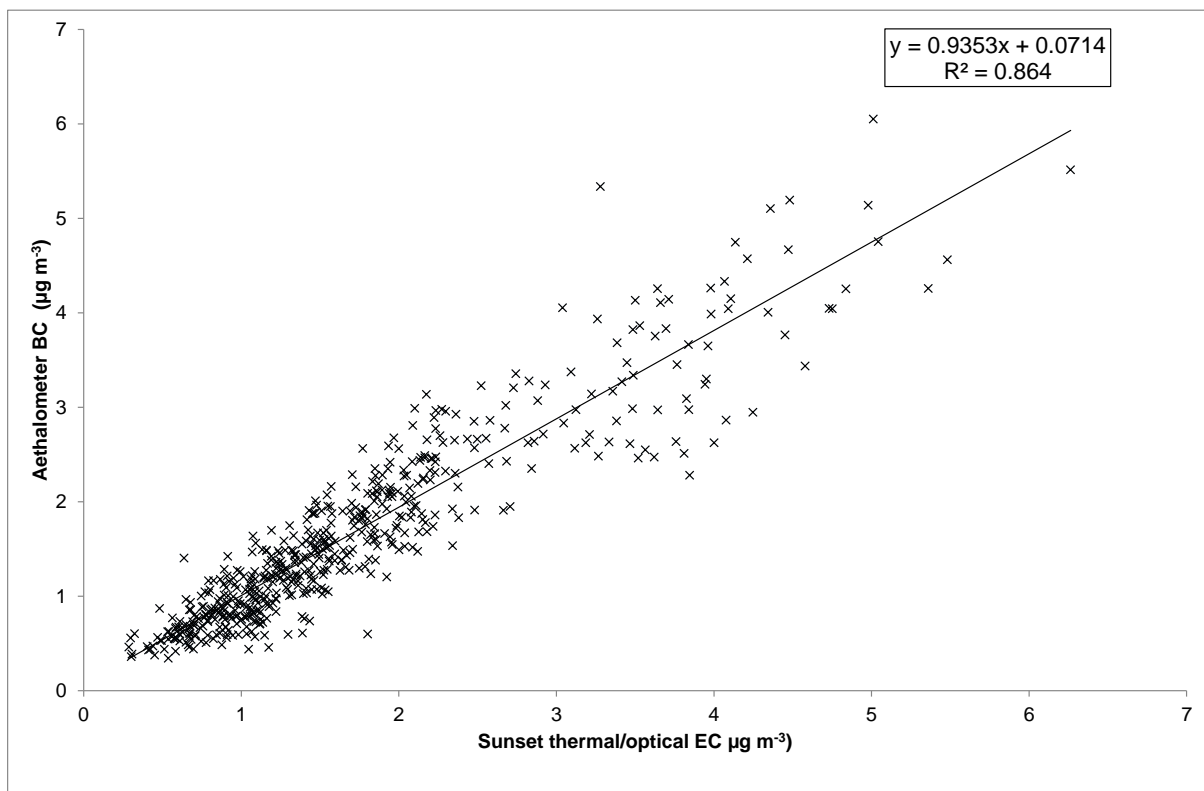
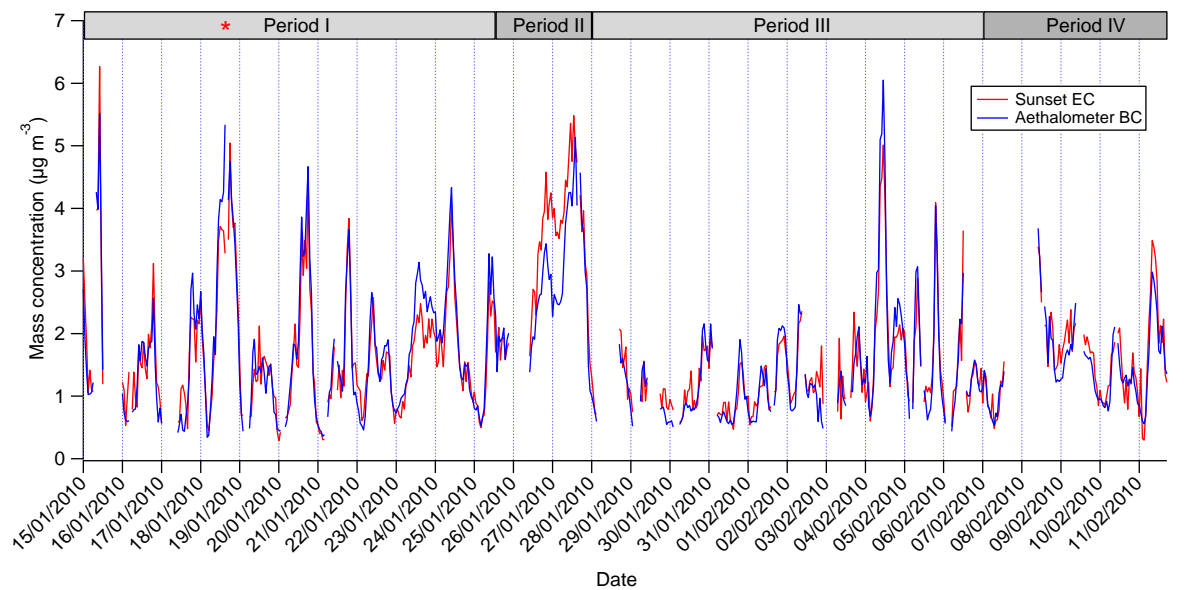


Fig. S9: Comparison of Sunset analyzer thermal/optical EC and aethalometer BC

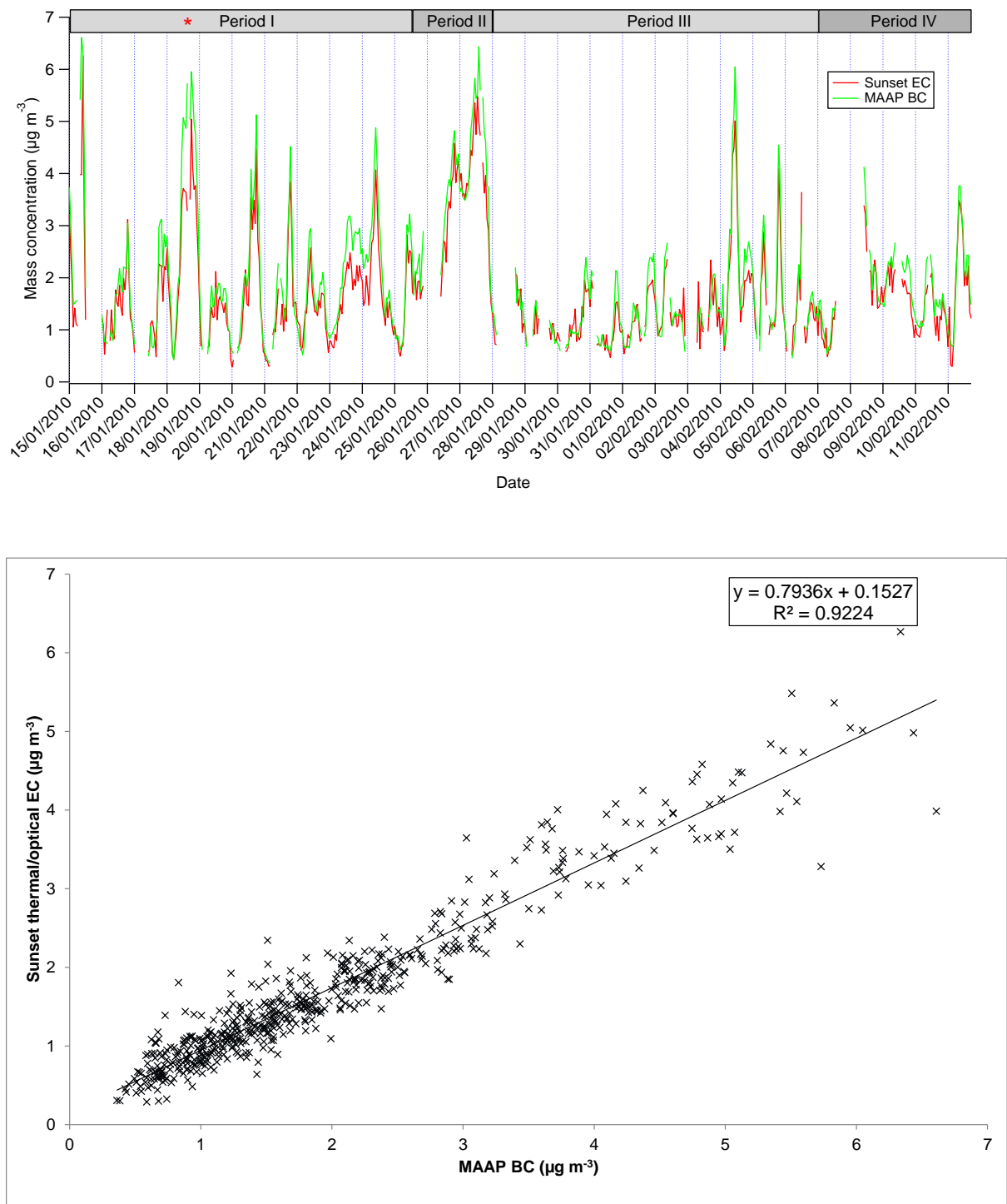


Fig. S10: Comparison of Sunset thermal/optical EC and MAAP BC

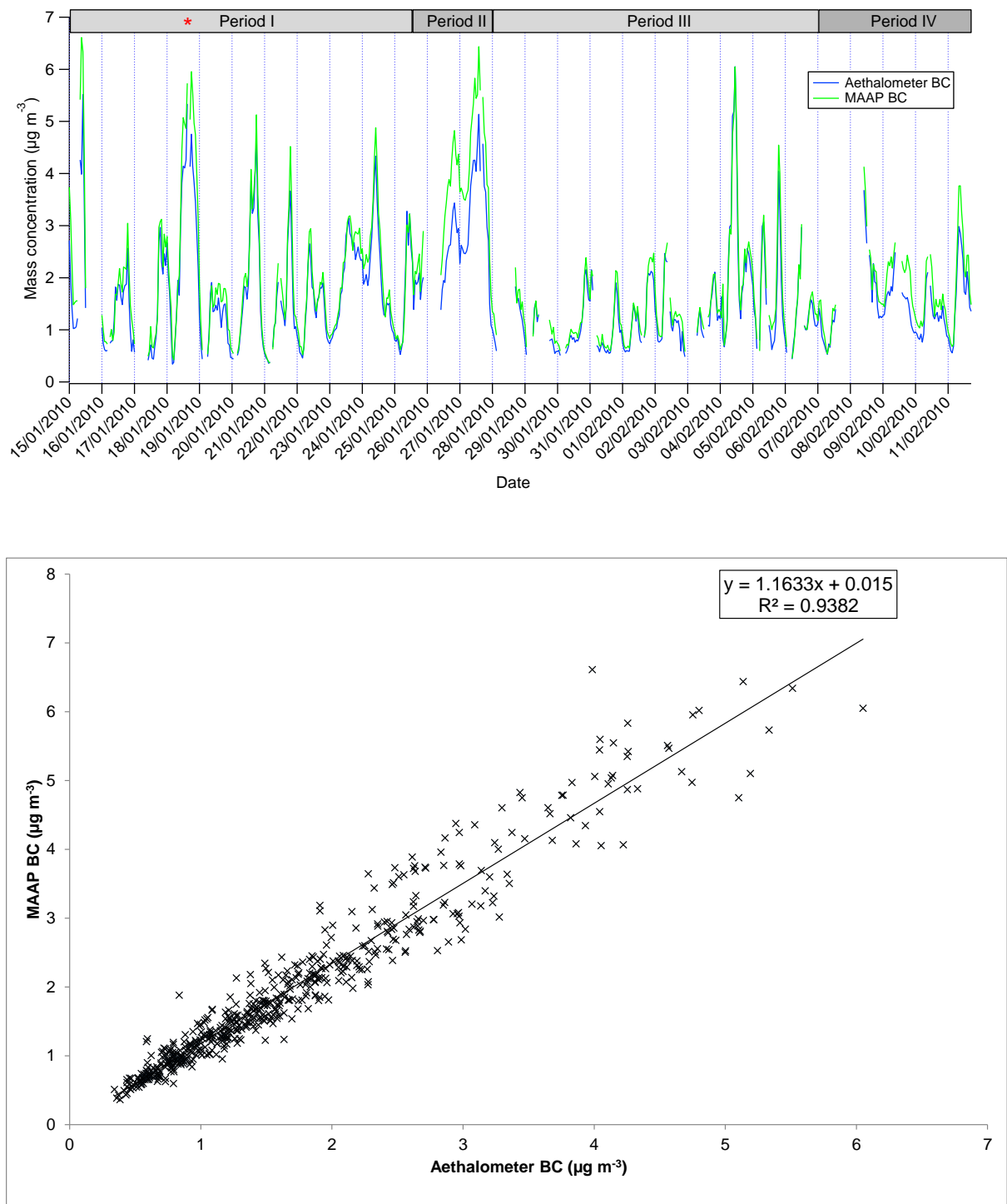


Fig. S11: Comparison of aethalometer BC and MAAP BC

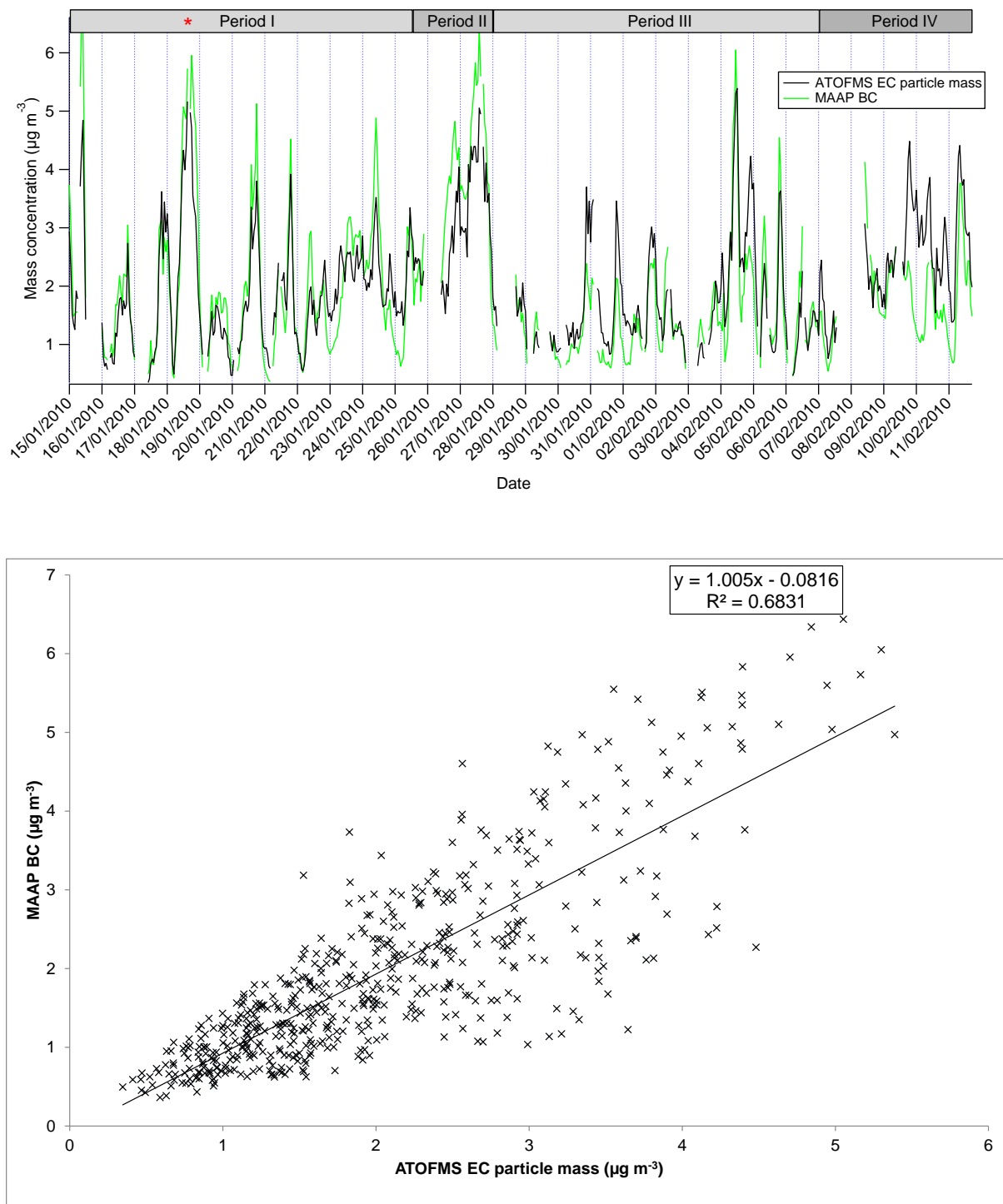


Fig. S12: Comparison of ATOFMS EC particle mass and MAAP BC

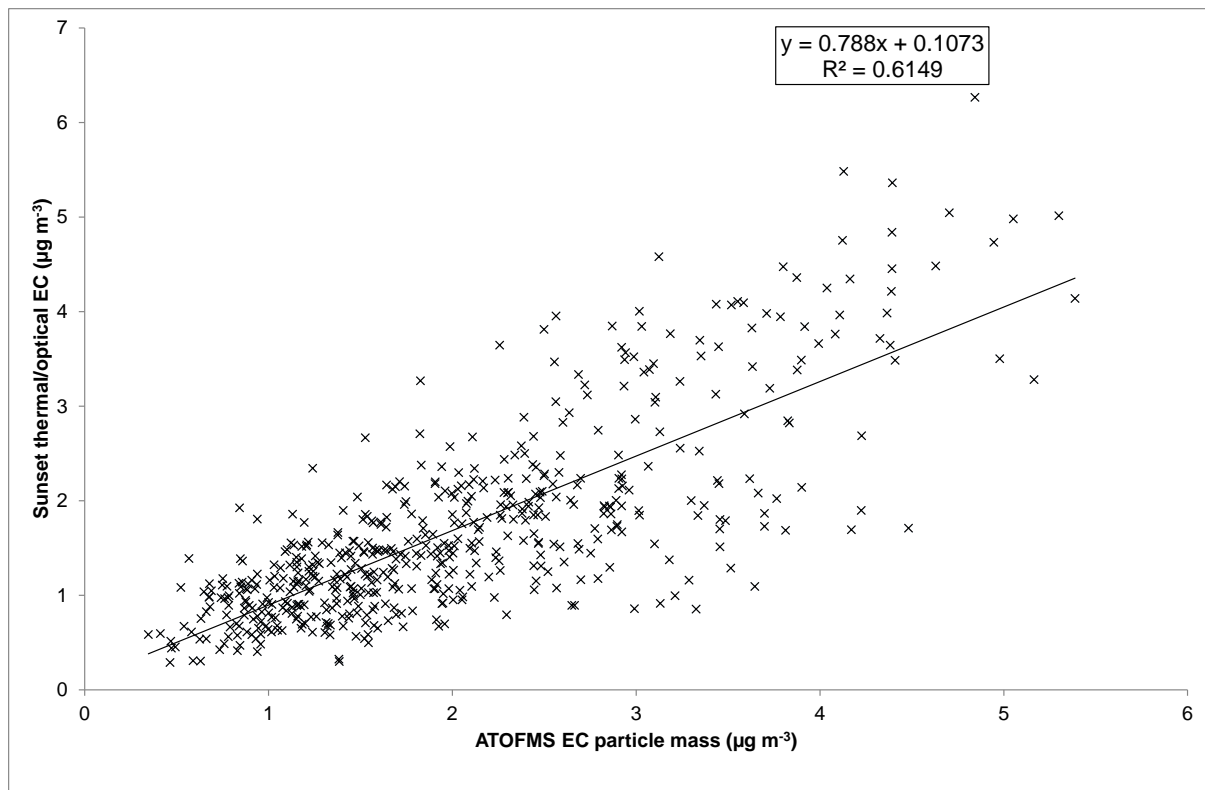


Fig. S13: Comparison of ATOFMS EC particle mass and Sunset thermal/optical EC.

Temporal trends are given in Fig. 7.

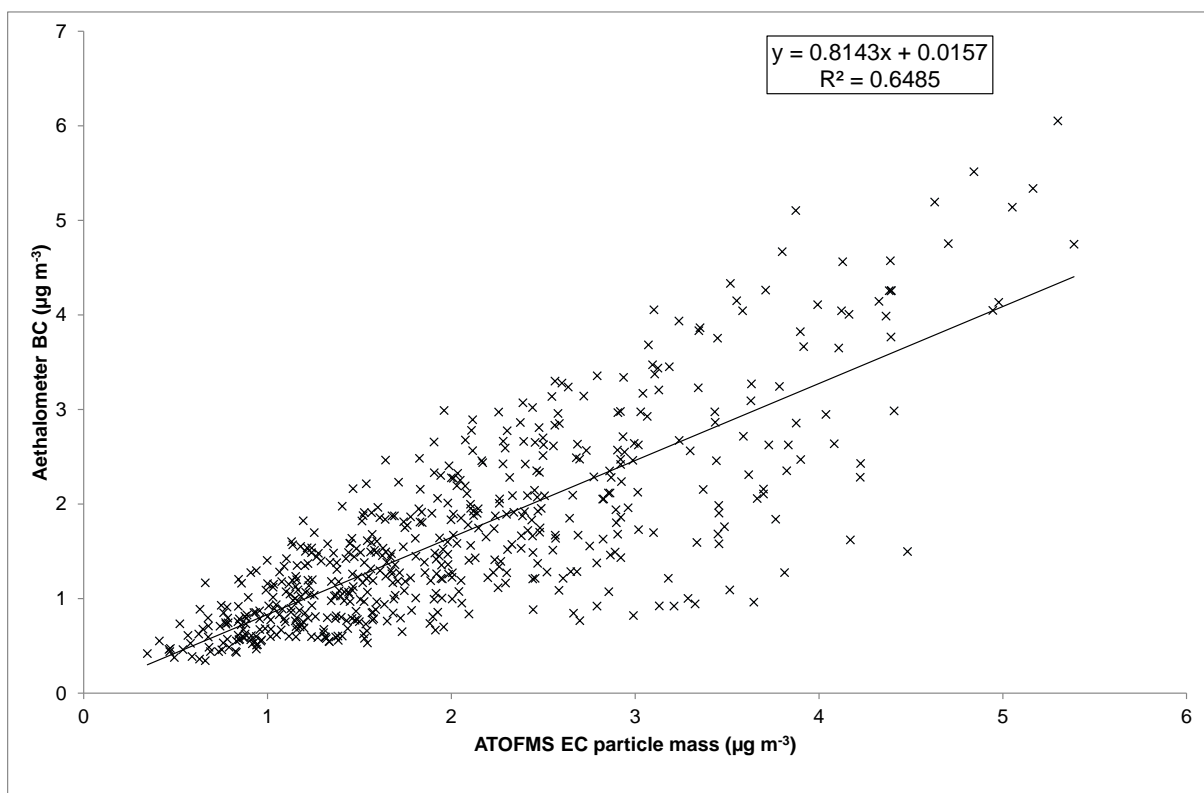
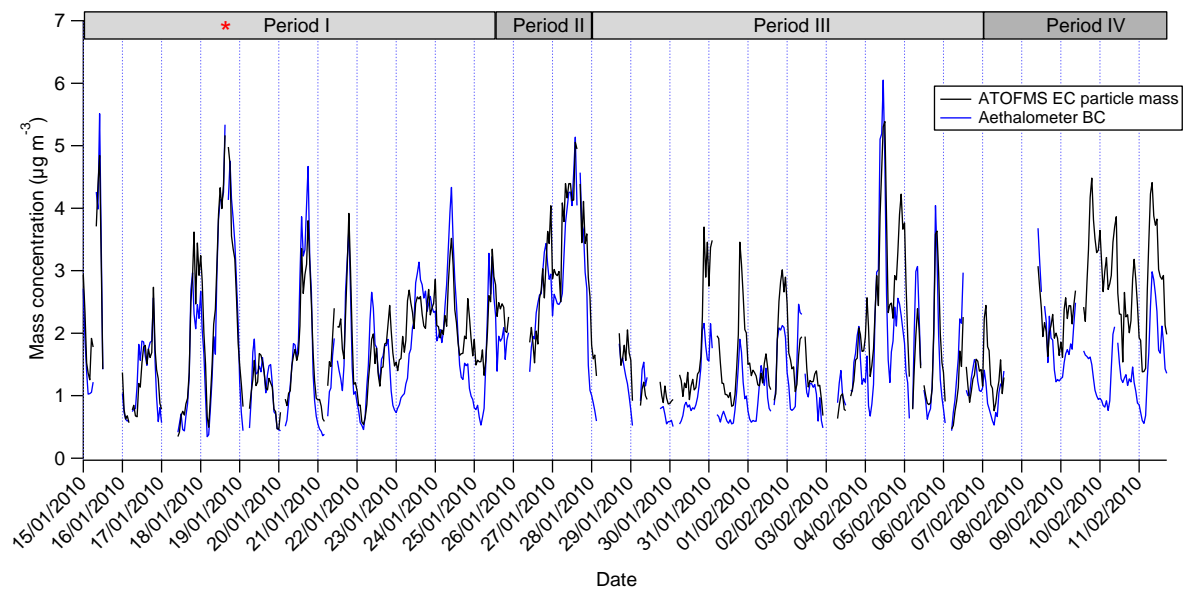


Fig. S14: Comparison of ATOFMS EC particle mass and aethalometer BC

Effect of varying particle density upon scaled mass concentration:

Particle densities of 1.3 and 1.7 g cm⁻³ have also been explored in order to investigate the effect of varying particle density upon the resultant mass concentrations obtained for ATOFMS EC particle mass (Figs. S15-18). In brief, using either 1.3 or 1.7 g cm⁻³ results in very little change to the temporality of the total scaled EC mass ($R^2 = 0.97$ and 0.98 respectively when compared to using a density 1.5). However, the slope and therefore mass concentration values are affected (slope = 1.02 and 0.78 for 1.3 and 1.7 g cm⁻³ respectively, when compared to a density of 1.5 g cm⁻³). Slightly higher mass concentrations are observed using a density of 1.3 g cm⁻³, and lower mass concentrations are observed using a density of 1.7 g cm⁻³. This effect arises because the density value is used to “convert” the aerodynamic diameter (d_{va}) to a corresponding mobility diameter (d_m) in order to scale the particle counts to the TDMPS data. For example, employing a higher density (1.7 g cm⁻³) requires the use of lower mobility diameter bins from the TDMPS compared to those used for a density of 1.5 g cm⁻³. The centroids of those smaller d_m bins are also used to estimate particle volume (assuming spherical shape), and thus the particle volume estimate for a density of 1.7 g cm⁻³ is lower than that obtained for a density of 1.5 g cm⁻³. When converting from volume to mass concentration, the volume is multiplied by the density and this offsets the effect of using smaller diameter bins for the volume calculations to an extent, but not completely. Ultimately, no single density value is perfectly suitable for such a calculation because different particle types will exhibit different particle densities. Although single density values have been demonstrated to work reasonably well for converting ATOFMS data to PM₁ mass concentrations (Qin et al., 2006), simultaneous measurement of d_{va} and d_m , or an optical scattering measurement of effective density for each particle remains the best way to tackle this problem, especially for non-spherical soot particles (DeCarlo et al., 2004; Moffet and Prather, 2009). In the absence of such measurements, the value of 1.5 g cm⁻³ has been chosen because it corresponds to the best estimate available for the bulk density of the particle ensemble for this campaign.

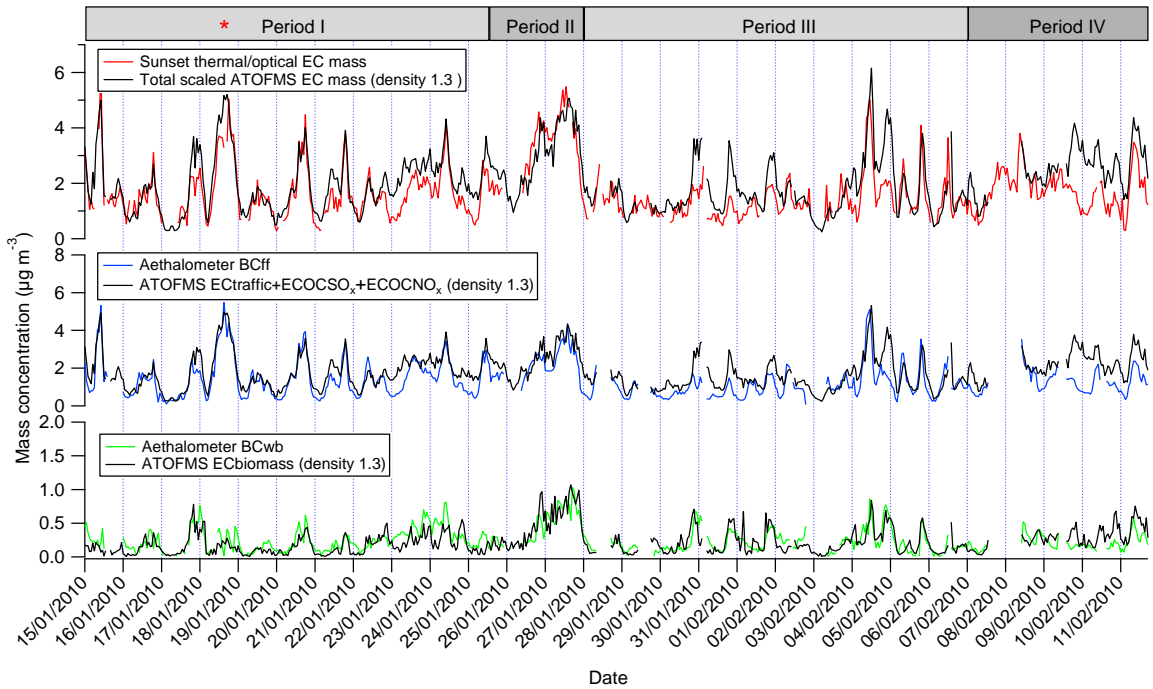


Fig. S15: Top: Comparison of total scaled hourly ATOFMS EC particle mass concentration (assuming a particle density of 1.3 g cm^{-3}) and hourly average Sunset thermal/optical EC mass concentration. Middle: Scaled ATOFMS mass concentration for the sum of ECtraffic, ECOC SO_x and ECOC NO_x (assuming a particle density of 1.3 g cm^{-3}) compared with hourly average modelled aethalometer BC_{ff} mass concentration. Bottom: Scaled ATOFMS mass concentration for ECbiomass (assuming a particle density of 1.3 g cm^{-3}) compared with hourly average modelled aethalometer BC_{bb} mass concentration.

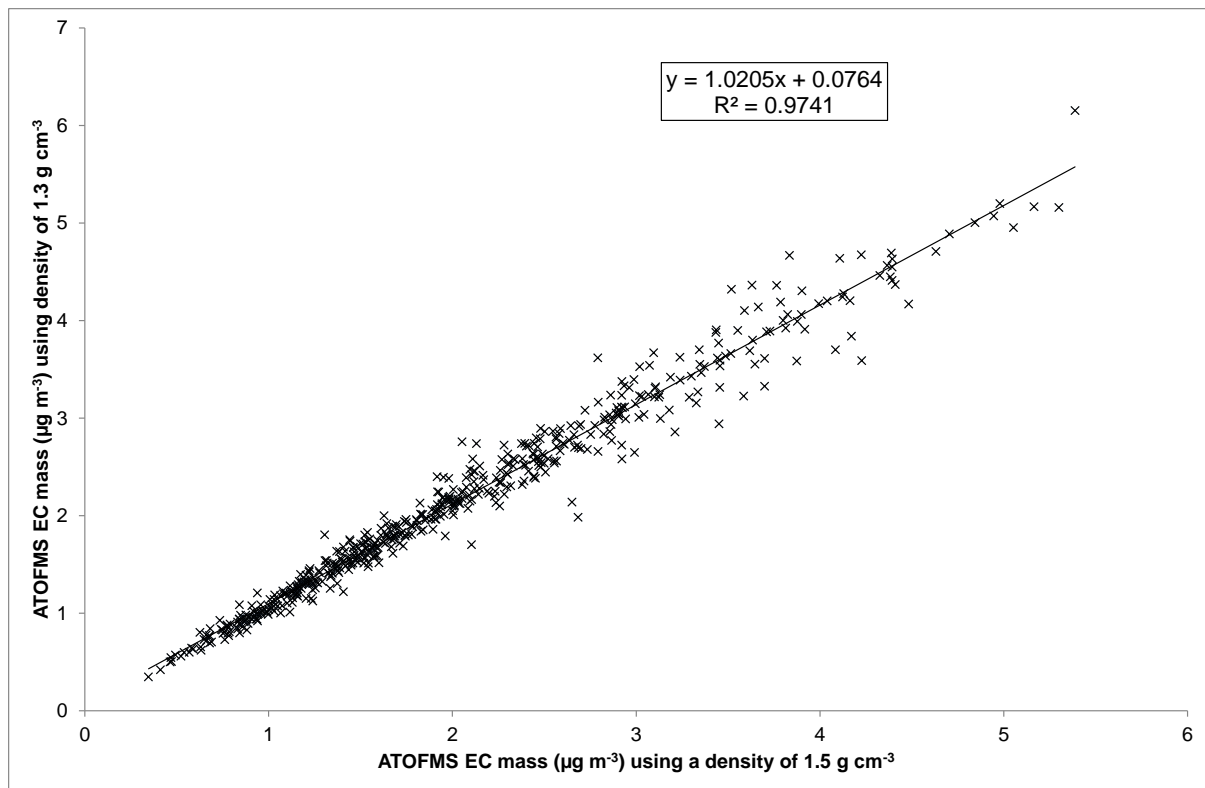


Figure S16: Comparison of ATOFMS scaled EC mass concentration derived using density values of 1.3 g cm^{-3} and 1.5 g cm^{-3} .

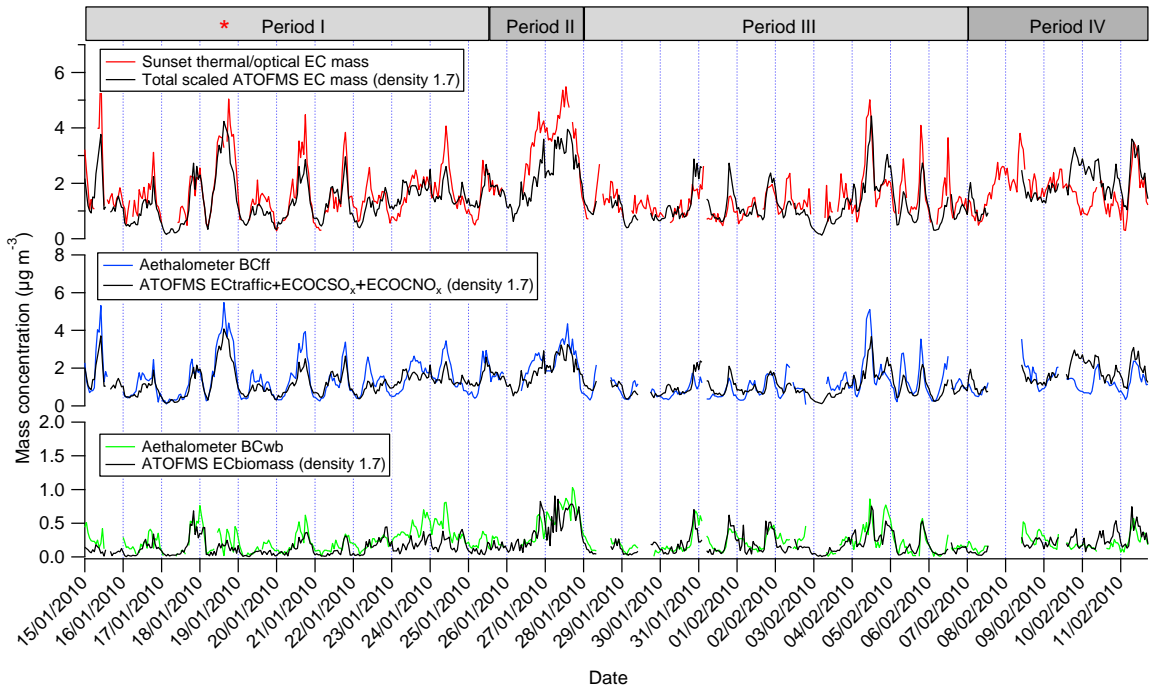


Fig. S17: Top: Comparison of total scaled hourly ATOFMS EC particle mass concentration (assuming a particle density of 1.7 g cm^{-3}) and hourly average Sunset thermal/optical EC mass concentration. Middle: Scaled ATOFMS mass concentration for the sum of ECtraffic, ECOC SO_x and ECOC NO_x (assuming a particle density of 1.7 g cm^{-3}) compared with hourly average modelled aethalometer BC_{ff} mass concentration. Bottom: Scaled ATOFMS mass concentration for ECbiomass (assuming a particle density of 1.7 g cm^{-3}) compared with hourly average modelled aethalometer BC_{bb} mass concentration.

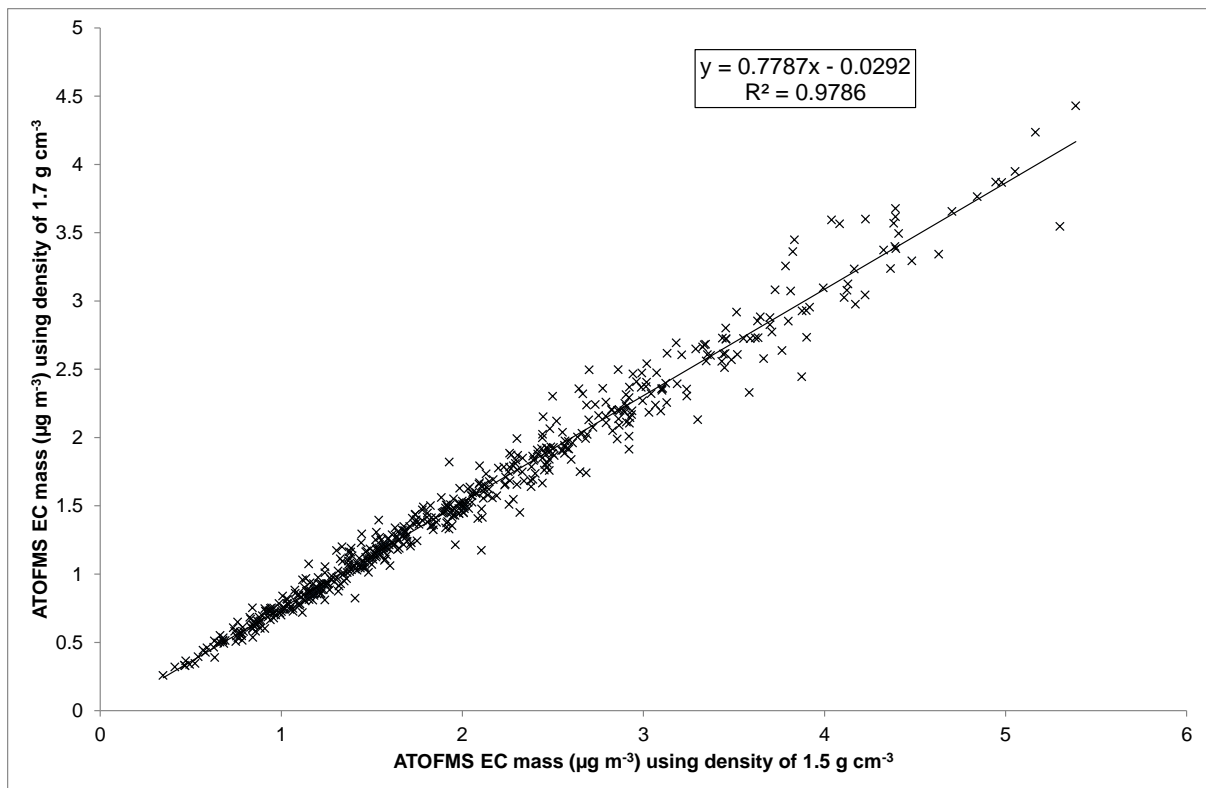


Figure S18: Comparison of ATOFMS scaled EC mass concentration derived using density values of 1.7 and 1.5 g cm⁻³.

References

- Birmili, W., Stratmann, F., and Wiedensohler, A.: Design of a DMA-based size spectrometer for a large particle size range and stable operation, *J. Aerosol Sci.*, 30, 549-553, 1999.
- DeCarlo, P. F., Slowik, J. G., Worsnop, D. R., Davidovits, P., and Jimenez, J. L.: Particle morphology and density characterization by combined mobility and aerodynamic diameter measurements. Part 1: Theory, *Aerosol Sci. Technol.*, 38, 1185-1205, 2004.
- Moffet, R. C., and Prather, K. A.: In-situ measurements of the mixing state and optical properties of soot with implications for radiative forcing estimates, *P. Natl. Acad. Sci.*, 106, 11872-11877, 2009.
- Pratt, K. A., Mayer, J. E., Holecek, J. C., Moffet, R. C., Sanchez, R. O., Rebotier, T. P., Furutani, H., Gonin, M., Fuhrer, K., Su, Y., Guazzotti, S., and Prather, K. A.: Development and Characterization of an Aircraft Aerosol Time-of-Flight Mass Spectrometer, *Anal. Chem.*, 81, 1792-1800, 2009.

Qin, X., Bhave, P. V., and Prather, K. A.: Comparison of Two Methods for Obtaining Quantitative Mass Concentrations from Aerosol Time-of-Flight Mass Spectrometry Measurements, *Anal. Chem.*, 78, 6169-6178, 2006.

Wenzel, R. J., Liu, D.-Y., Edgerton, E. S., and Prather, K. A.: Aerosol time-of-flight mass spectrometry during the Atlanta Supersite Experiment: 2. Scaling procedures, *J. Geophys. Res.*, 108, 8427, 10.1029/2001JD001563, 2003.